

## Giant Electron Tails and Passing Electron Pinch Effects in Tokamak-Core Turbulence

K. Hallatschek

*Centre for Interdisciplinary Plasma Science, Max-Planck Institut für Plasmaphysik, EURATOM-IPP Association, D-85748 Garching, Germany*

W. Dorland

*Department of Physics, University of Maryland, College Park, Maryland 20742, USA*

(Received 7 July 2004; published 26 July 2005)

The anomalous particle transport in a tokamak core is believed to be linked to the advection of magnetically trapped electrons alone, owing to the passing electrons maintaining a thermal equilibrium along the field lines. Surprisingly, in nonlinear numerical studies, the radial flux of passing electrons rivals that of the trapped ones. The strong interaction of passing electrons and electric fluctuations is mediated by long tails of the modes along the magnetic field, which are generated by the passing electrons in the first place.

DOI: [10.1103/PhysRevLett.95.055002](https://doi.org/10.1103/PhysRevLett.95.055002)

PACS numbers: 52.35.Ra, 52.55.Fa, 52.65.Tt

*Introduction.*—The anomalous diffusion in a tokamak core is believed to be dominated by turbulence around ion Larmor radius scales, e.g., due to the ion temperature gradient (ITG) or trapped electron instabilities. For such modes the comparatively fast thermal electron motion along the magnetic field lines tends to force the electric potential to be proportional to the density fluctuations on each flux surface. This electron response is usually called “adiabatic”. Small deviations from this response are called “nonadiabatic”. The ion density is forced by quasineutrality to follow the electron density up to a tiny amount responsible for the electric field. Consequently, the fluctuating radial  $\mathbf{E} \times \mathbf{B}$ -drift velocity, as a derivative of the electric potential, is  $90^\circ$  out of phase with the density. This makes the turbulence-induced radial particle flux much smaller than, e.g., the heat flux. Only the minority of electrons which either have rather low kinetic energy or are trapped by magnetic mirror forces on the outboard side of the torus can contribute to the particle transport. Thus, the direction of transport is not determined by the overall density gradient but by the gradient in the small region in phase space susceptible to turbulent diffusion, which for sufficiently high electron temperature gradient, can have reversed sign and cause inward particle transport (pinch).

The particle flux has been estimated using a theoretical ansatz for the nonadiabatic part of the fluctuating electron density with an essentially unchanged ion mode. For ITG modes this has been done for fluid electrons in slab geometry [1] (the ion mixing mode), for collisionless, freely passing electrons and toroidal geometry [2,3], and for trapped electrons [4], with the general conclusion that the radial flux of passing electrons is negligible in the core, since their nonadiabatic response is rather well suppressed by the high parallel electron phase mixing frequency  $v_e k_{\parallel} \sim \sqrt{m_i/m_e} \omega \sim 60\omega$  in comparison to the mode frequency  $\omega$ , whereas the trapped electron fraction is still of order  $\sqrt{\epsilon} = \sqrt{r/R} \sim 0.3$  for a tokamak. (For particle type

$\sigma$ ,  $v_\sigma = \sqrt{T_\sigma/m_\sigma}$ , while  $T_\sigma$ ,  $m_\sigma$ , and  $q_\sigma$  are the temperature, mass, and signed charge. The minor and major tokamak radius are  $r$ ,  $R$ , and  $k_{\parallel}$  is the typical mode wave number along the field lines.) On these premises, several comprehensive turbulence models [5,6] neglect the majority of passing electrons.

Surprisingly, the nonlinear gyrokinetic turbulence studies reported here demonstrate that the contribution from the passing electrons can instead be quite strong and produce an overall inward particle transport, even when the trapped electrons are transported outward. The cause is that the passing electrons augment the ion scale mode with a very extended “tail” along the magnetic field. This electron tail in turn has a relatively small phase mixing frequency  $k_{\parallel} v_e$  and therefore affects the passing electrons already at zeroth order in  $1/v_e$ . The existence and consequences of such perturbations have not been previously considered. Our analysis indicates that the justification for regarding the passing electrons as a small perturbation breaks down and a significant particle transport due to them is possible.

*Numerical results.*—The mentioned phenomena have been discovered in gyrokinetic turbulence computations with the GS2 code [7] for various parameter sets inspired by Tore Supra discharges in helium [8]. As a specific example we use  $q = 1.8$ ,  $s = r/q(dq/dr) = 0.5$ ,  $\epsilon = 0.13$ ,  $R/L_n = 3.4$ ,  $R/L_{T_i} = 5$ ,  $R/L_{T_e} = 10$ , and collision frequencies  $\nu_e = 0.49\nu_i/R$ ,  $\nu_i = 0.11\nu_i/R$  corresponding to the normalized detrapping rates  $\nu_e^* = 0.31$ ,  $\nu_i^* = 4.2$ . The gradient lengths are defined as  $L_\xi = -\xi/(d\xi/dr)$ , the safety factor  $q$  is the number of toroidal turns per poloidal turn of a magnetic fieldline. These dimensionless parameters (apart from the ion collisions) represent the dimensional parameters  $T = 2.4$  keV,  $n = 5 \times 10^{19}$  m $^{-3}$ ,  $R = 2.28$  m,  $r = 0.30$  m. To demonstrate the relevance of our findings to the majority of fusion experiments, we alter these parameters slightly, taking locally  $T_i = T_e$  and

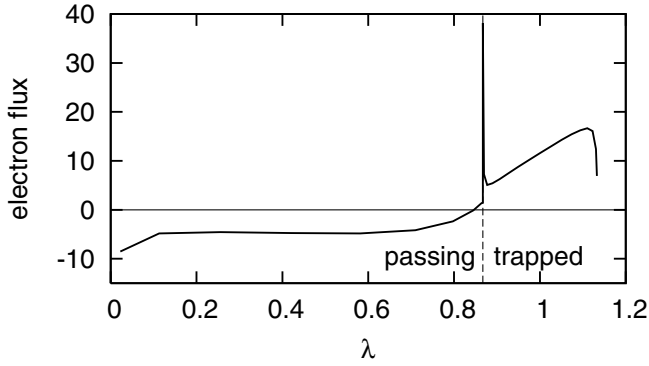


FIG. 1. Turbulent radial electron flux versus the customary pitch angle parameter  $\lambda = \mu B_0/E$ , with the magnetic moment  $\mu = m_e v_\perp^2/(2B)$  and the kinetic energy  $E = m_e v^2/2$ . The normalization is such that the integral of the curve is the dimensionless particle flux.  $B_0$  is the reference magnetic field.

considering a deuterium instead of a helium plasma. The numerical saturated turbulent ion/electron heat flux and the particle flux were, respectively,  $Q_i = 16nT\rho_i^2 v_i/R^2$ ,  $Q_e = 22nT\rho_i^2 v_i/R^2$ ,  $\Gamma = -0.5n\rho_i^2 v_i/R^2$ , with ion Larmor radius  $\rho_i = \sqrt{m_i T_i}/(q_i B)$ . While the inward particle transport may not be surprising at the relatively high temperature gradients driving the turbulence, the contributions from trapped and passing electrons shown in Fig. 1 are: the contribution from the passing electrons is not only significant, it is actually outweighing the one from the trapped electrons and pinching the particles. This is a novel numerical result. In the remainder of this Letter, we attempt to elucidate the underlying physical mechanism. We begin by considering the salient features of the linear eigenmodes.

This behavior persists for the quasilinear transport of the dominant linear eigenmode at a poloidal wave number  $k_\theta \rho_i = 0.5$ , which is shown as case (a) in Table I and the top half of Fig. 2. (The quasilinear flux is defined below.) The mode exhibits a striking tail about 17 poloidal turns long. With an amplitude of 50% of the central part of the mode, it is the dominant feature of the mode. The length of the tail suggests that the passing electrons are not a small perturbation, since their parallel length scale  $v_e/(\omega q R) \sim 60$  is the only one large enough.

TABLE I. Table of linear runs; the unit of frequency is  $v_i/R$ , of heat flux is  $nT\rho_i^2 v_i/R^2$ , of particle flux  $n\rho_i^2 v_i/R^2$ ; the fluxes are normalized to  $|\phi(\theta = 0)|^2$ .

$\epsilon$	$v_e$	$v_i$	$R/L_n$	$R/L_{T_e}$	$R/L_{T_i}$	adiabatic curvature		$\omega$	$Q_e$	$Q_i$	$\Gamma/Q_e$	case
						ions	drifts					
0.13	0.49	0.11	3.37	10	5	no	on	$0.498 + 0.560i$	1.7	0.10	-0.015	a
0	0.49	0.11	3.37	10	5	no	on	$0.454 + 0.215i$	1.8	0.078	-0.0075	b
0	0	0	3.37	10	5	no	on	$0.330 + 0.257i$	2.3	0.039	-0.010	c
0	0	0	3.37	10	5	no	off	$0.573 + 0.167i$	1.3	0.10	0.019	d
0	0	0	1	15	5	no	off	$1.233 + 0.500i$	1.4	0.017	-0.0029	e
0.13	0.49	0.11	3.37	10	3.5	no	on	$0.623 + 0.620i$	1.6	0.10	0.021	f
0.13	0.49	0.11	3.37	10	5	yes	on	$0.526 + 0.464i$	1.9	0	0	g

Switching off particle trapping by letting  $\epsilon \rightarrow 0$  [case (b)], and eliminating the collisions [case (c)] changes neither the sign of the real frequency nor the basic features of the mode. The particle flux and electron heat flux are still of similar magnitude (Table I), although they are then manifestly carried exclusively by the passing electrons. As a last step, even removing the curvature drift completely [case (d)], results in a mode with the same properties. This supports the view that the mechanism responsible for the pronounced tails is still present in the simplified scenario. [For (d), the tail is significantly longer, since the curvature terms provide an effective cutoff. Moreover, due to a slight change in the balance between inward and outward flowing electrons the particle flux does change from inward to outward. This is understood, since the curvature had reduced the effective density gradient parameter  $1/L_n$  on the outboard midplane by  $2/R$ . The inward flux can be recovered, by changing the density gradient to  $R/L_n = 1$  and the electron temperature gradient to  $R/L_{T_e} = 15$  (e).]

*Collisionless electron tail.*—Judging from the robustness of the basic mode features, it seems adequate to investigate the electron response to the ion fluctuations for singly charged ions, neglecting trapping, collisions, finite electron gyro radius, and curvature effects on the electrons. We normalize all quantities, so that the background density, temperature, and magnetic field,  $n_0$ ,  $T_0$ ,  $B_0 = 1$ , and the particle charge  $q_{e/i} = \mp 1$ . The density fluctuations,  $n$ , are identical for electrons and ions as required by quasineutrality.

An indicator of one of the species not being in thermal equilibrium on a magnetic fieldline is the deviation of the density and electric potential from the respective adiabatic (or Boltzmann) relation. Especially instructive are the quantities

$$2\phi_{e/i} \equiv \phi + \frac{nT_0}{n_0 q_{e/i}}, \quad (1)$$

since they partition the electric potential into an ion and an electron component,  $\phi = \phi_e + \phi_i$ .

For the linear eigenmode of the standard case (a), the real parts of  $\phi_e$  and  $\phi_i$  are shown in the lower half of Fig. 2. Only the central part of the potential is affected by the ion fluctuations,  $\phi_i$ . For  $|\theta| \gtrsim 2\pi$ , the radial wavelength

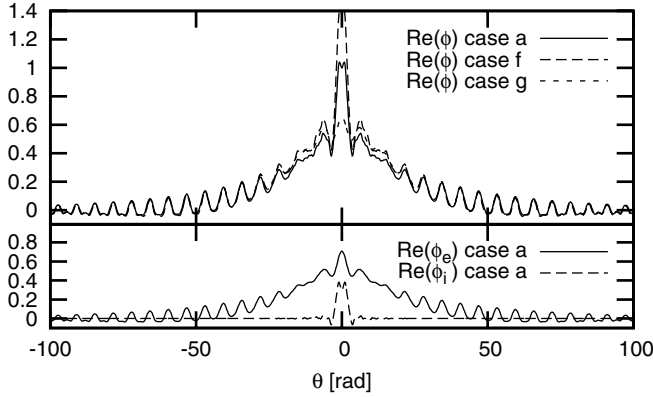


FIG. 2. Top:  $\text{Re}[\phi(\theta)]$  of the linear mode structures along a fieldline versus the poloidal angle  $\theta$ , bottom: electron and ion component  $\text{Re}(\phi_{e/i})$  case (a). The reference case (a) is normalized to  $\phi(\theta = 0) = 1$ , the other cases are normalized to (a) according to the tail amplitudes.

$2\pi/(s\theta k_\theta)$  starts to become smaller than the ion Larmor radius, and the ions average over the potential fluctuations during one gyration, enforcing a Boltzmann response. The electron component  $\phi_e$  does not show the strong peaking close to  $\theta = 0$  due to the rapid phase mixing of the electrons over short scales along the magnetic field. (Both of these effects can of course be derived formally from the gyrokinetic equations [9].) Apparently, the giant tail is caused by the electron fluctuations.

To track down the large amplitude of the electron contribution, we consider the drift-kinetic equation [10]

$$\partial_t h_e + v_\parallel \partial_\parallel h_e + [F_0(v/v_e)/v_e^3](i\omega_* \phi + \partial_t \phi) = 0, \quad (2)$$

for the nonadiabatic part,

$$h_e(\mathbf{v}) \equiv f_e(\mathbf{v}) - [F_0(v/v_e)/v_e^3]e\phi/T_0, \quad (3)$$

of the fluctuations  $f_e$  of the electron distribution function, with  $i\omega_* = -ik_\theta[n'_0 + T'_0(v^2/v_e^2 - 3)/2]$  representing the background density and temperature gradient, and  $F_0(v) \equiv \exp(-v^2/2)/(2\pi)^{3/2}$  being the background Maxwell-distribution of the electrons.

Fourier transforming (2) along the fieldlines results in a formal solution for the electron response to the ion fluctuations,

$$h_e(\mathbf{v}, k_\parallel) = \frac{\omega_* - \omega}{\omega - k_\parallel v_\parallel} [F_0(v/v_e)/v_e^3] \phi(k_\parallel). \quad (4)$$

Integration of  $h_e$  over velocity space, applying the definitions (1) and (3), and transforming from the integration variable  $\mathbf{v}$  to  $\boldsymbol{\nu} \equiv \mathbf{v}/v_e$  yields

$$\begin{aligned} \phi_e(k_\parallel) &= \int h_e(\mathbf{v}, k_\parallel) d^3 v \\ &= \int \frac{\omega_* - \omega}{\omega - k_\parallel v_e \nu_\parallel} F_0(\nu) \phi(k_\parallel) d^3 \nu \\ &\equiv R(k_\parallel v_e) \phi(k_\parallel), \end{aligned} \quad (5)$$

with the then defined integral response kernel  $R(k_\parallel v_e)$ . With (1), this results in a closed system for the electron perturbation  $\phi_e$ ,

$$\phi_e(k_\parallel) = R(k_\parallel v_e) [\phi_e(k_\parallel) + \phi_i(k_\parallel)]. \quad (6)$$

Following the customary procedure, assuming near-adiabaticity of the electrons,  $\phi_e \ll \phi_i$ , Eq. (6) is solved by expanding

$$\phi_e(k_\parallel) = \phi_{e1} + \phi_{e2} + \dots, \quad (7)$$

where the individual terms are computed by iterative application of the electron response formula in Eq. (5) to the  $\phi$  perturbations, i.e.,  $\phi_{e,n+1} = R(k_\parallel v_e) \phi_{e,n}$ ,  $\phi_{e1} = R(k_\parallel v_e) \phi_i$ . The justification for this is that, assuming a typical parallel wave number  $k_{\parallel,0} \approx 1/(qR)$  for the mode, due to Eqs. (4) and (5),  $R(k_\parallel v_e) \sim \alpha \equiv \omega/(k_\parallel v_e) \sim \sqrt{m_e/m_i} \sim 1/60$ . Each term in the series is expected to be smaller than the previous one by a factor  $\alpha$ .

Knowing  $\phi_e$ ,  $\phi_i$ , the quasilinear particle flux can be computed by  $\Gamma = \text{Re}(\langle n^* v_r \rangle) = \text{Re}(\langle n^* ik_\theta \phi \rangle) = -2k_\theta \text{Im}(\langle \phi_e^* \phi_i \rangle)$ , where  $v_r$  is the radial  $\mathbf{E} \times \mathbf{B}$  velocity, and  $\langle \rangle$  the flux surface average.

With the rather low  $\alpha$ , according to Eq. (4) resonant contributions to  $\Gamma$  can come only from rather slow electrons. For a sufficiently large electron temperature gradient, these electrons have a reversed radial phase space density gradient, whose turbulent erosion leads to the inward particle flux of the ion mixing mode [1,3].

However, this computation is neglecting the small- $k_\parallel$  Fourier components of  $\phi$ , which are conspicuous from the appearance of the giant tails in the first place, and for which  $R(k_\parallel v_e)$  may be appreciable ( $k_\parallel v_e \lesssim 1$ ), as seen in a plot of the analytically computed  $R(k_\parallel v_e)$  for cases (a) and (d) in Fig. 3. One may still hope that, even if for certain  $k_\parallel$  the series (7) does not properly converge, the affected parallel wave numbers are unimportant for the quasilinear particle transport. But this can be disproved by formally computing the quasilinear particle flux due to the individual terms in (7),

$$\begin{aligned} \Gamma_n &= -2k_\theta \text{Im} \int \phi_{e,n} \phi_i^* dk_\parallel \\ &= -2k_\theta \text{Im} \int R(k_\parallel v_e)^n |\phi_i(k_\parallel)|^2 dk_\parallel \\ &= \frac{-2k_\theta}{v_e} \text{Im} \int R(k')^n \left| \phi_i\left(\frac{k'}{v_e}\right) \right|^2 dk'. \end{aligned} \quad (8)$$

Since, for large  $k'$ ,  $R(k')^n = O(1/k'^n)$ , for  $n \geq 2$  contributions from  $k' \lesssim 1$  with  $R(k') = O(1)$  dominate in the integral. Hence, in the interesting limit  $\alpha \rightarrow 0$ ,  $v_e \rightarrow \infty$  one can approximate  $|\phi_i|^2(k'/v_e) \approx |\phi_i|^2(0)$ , and obtain  $\Gamma_n = O(1/v_e) k_\theta |\phi_i(0)|^2 = O(\alpha) k_\theta |\phi_i(0)|^2$ , which is independent of the expansion order  $n$ . In other words, due to the tail, the overall effect of the  $\phi_{e,n}$  on the passing electrons does not decrease with  $n$  and each contribution is of the same order as that of  $\phi_{e,0}$ . Transforming back to configu-

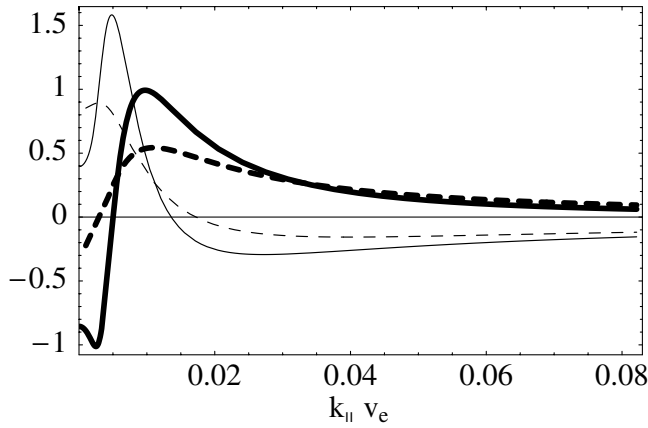


FIG. 3. Real (thick) and imaginary (thin) part of  $R(k_{\parallel}v_e)$  for cases (d) (solid lines) and (a) (dashed lines) in Table I. (The unit of the dedimensionalized  $k_{\parallel}v_e$  is  $v_i/R$ .)

ration space along the field lines, the series  $\phi_e = \sum \phi_{e,n}$  either does not converge at all, if  $R(k_{\parallel}v_e) > 1$  for some  $k_{\parallel}$ , or the first term does not give a reliable estimate for  $\phi_e$ , since  $\alpha \ll 1$  does not imply  $R(k_{\parallel}v_e) \ll 1$  for all  $k_{\parallel}$ .

*Giant electron tails and numerical evidence.*—Because of the unreliability of the expansions (7) and (8), it is better to consider the weak coupling of a *self-consistent* electron mode of low parallel wave number and an ion mode localized near  $\theta = 0$  on equal grounds. Particularly interesting, and unexpected by the earlier treatments, is the situation of a dominant electron mode inducing a giant electron tail in our reference case. According to the foregoing discussion this should correspond to a near-breakdown of the series expansion (8) caused by  $R \rightarrow 1$  near a certain resonant  $k_{\parallel}$ . That turns indeed out to be quite accurately true for the simplified linear case (d) as shown in Fig. 3. For the complete physics case (a), the kernel  $R$  is approaching one, up to  $|R - 1| \approx 1/2$ . (For parameters without strong tails, the numerical solutions yield  $\text{Re}[R(k_{\parallel})] < 0$  at  $k_{\parallel}$  with  $\text{Im}[R(k_{\parallel})] = 0$ .)

In comparison with the dominant tail, the ion perturbations can be regarded as a small perturbation. Therefore, the mode frequency should be close to the tail resonance, independent of the ion parameters, while the quasilinear particle flux is now determined by the ion response to the tail. This is confirmed by further linear runs where the reference parameters of case (a) were modified into case (f) (ion temperature gradient lowered to  $R/L_{T_i} = 3.5$ ) and (g) (adiabatic ions,  $h_i, \phi_i \equiv 0$ ). Both frequencies (Table I) agree well with the one of case (a). The shape of the mode tails (dashed lines in Fig. 2 upper plot) is virtually identical. Yet the central ion affected part of the mode changes together with the particle flux, both being eliminated in the adiabatic ion case (g).

Increasing the ion temperature gradient at first changes only the central part of the modes (and the quasilinear particle flux) whereas the frequency is pinned at what is presumably the tail resonance frequency. For still higher  $T_i$  gradients, the fastest growing mode switches to a real frequency that makes more efficient use of the ion temperature gradient instead of the electron temperature gradient, and the tail resonance is lost.

*Conclusions.*—The breakdown of the assumption  $\omega/k_{\parallel}v_e \ll 1$  due to the electron tail (not necessarily a giant one) in the electric potential invalidates simple perturbative approaches, where the passing electron perturbations are assumed to be a weak perturbation generated by the central ( $|\theta| \lesssim 2\pi$ ) part of the potential stemming from the ions. The passing electrons must be treated consistently with the very extended (along the fieldline) electric potential perturbations, which they cause.

Different from conventional wisdom, the tail can be the dominant part of microinstability eigenfunctions, even in cases for which the poloidal wavelengths are large compared to the ion Larmor radius ( $k_{\theta}\rho_i < 1$ ). When this occurs, the roles of ions and electrons are reversed. The passing electrons determine the frequency of the mode, while the small nonadiabatic ion response determines the sign and magnitude of the particle flux.

A direct consequence of these results is that numerical simulations of anomalous particle transport induced by long wavelength microturbulence should generally resolve structures with  $k_{\parallel} \sim \omega_*/v_{te} \sim (\rho_e/L_{n,T})k_{\theta}$ . In addition, the simulation algorithm should recover the nearly adiabatic ion response for  $k_{\perp}\rho_i \gg 1$ —a challenging requirement for nonspectral or particle in cell algorithms.

This research was supported by the United States Department of Energy, under Contract Nos. DE-FG02-93ER54197, DE-FG02-02ER54675, and DE-FC02-04ER54784. Some of the computations were performed at NERSC.

- 
- [1] B. Coppi and C. Spight, Phys. Rev. Lett. **41**, 551 (1978).
  - [2] T. Antonsen, B. Coppi, and R. Englade, Nucl. Fusion **19**, 641 (1979).
  - [3] G. S. Lee and P. H. Diamond, Phys. Fluids **29**, 3291 (1986).
  - [4] A. S. Ware and P. W. Terry, Phys. Plasmas **1**, 658 (1994).
  - [5] M. A. Beer and G. W. Hammett, Phys. Plasmas **3**, 4018 (1996).
  - [6] X. Garbet *et al.*, Phys. Rev. Lett. **91**, 035001 (2003).
  - [7] M. Kotschenreuther, G. Rewoldt, and W. M. Tang, Comput. Phys. Commun. **88**, 128 (1995).
  - [8] G. T. Hoang *et al.*, Phys. Plasmas **10**, 405 (2003).
  - [9] E. A. Frieman and L. Chen, Phys. Fluids **25**, 502 (1982).
  - [10] See, e.g., J. A. Wesson, *Tokamaks* (Oxford University, Oxford, England, 1996), Chaps. 2.11 and 8.3.